BRAIN RESEARCH 1359 (2010) 44–55

available at www.sciencedirect.com

ScienceDirect

www.elsevier.com/locate/brainres

BRAIN RESEARCH

Research Report

# Synapse-to-neuron ratio is inversely related to neuronal density in mature neuronal cultures

D. Kacy Cullen[a,*,1], Meghan E. Gilroy[b,1], Hillary R. Irons[b], Michelle C. LaPlaca[b]

[a]Department of Neurosurgery, University of Pennsylvania, Philadelphia, PA, USA
[b]Coulter Department of Biomedical Engineering, Georgia Institute of Technology/Emory University, Atlanta, GA, USA

ARTICLE INFO

*Article history:*
Accepted 19 August 2010
Available online 25 August 2010

*Keywords:*
Synapse
Neuron
Cell culture
Synapsin
Tau
*In vitro*
Mature
Cell density

ABSTRACT

Synapse formation is a fundamental process in neurons that occurs throughout development, maturity, and aging. Although these stages contain disparate and fluctuating numbers of mature neurons, tactics employed by neuronal networks to modulate synapse number as a function of neuronal density are not well understood. The goal of this study was to utilize an *in vitro* model to assess the influence of cell density and neuronal maturity on synapse number and distribution. Specifically, cerebral cortical neurons were plated in planar culture at densities ranging from 10 to 5000 neurons/mm$^2$, and synapse number and distribution were evaluated via immunocytochemistry over 21 days *in vitro* (DIV). High-resolution confocal microscopy revealed an elaborate three-dimensional distribution of neurites and synapses across the heights of high-density neuronal networks by 21 DIV, which were up to 18 μm thick, demonstrating the complex degree of spatial interactions even in planar high-density cultures. At 7 DIV, the mean number of synapses per neuron was less than 5, and this did not vary as a function of neuronal density. However, by 21 DIV, the number of synapses per neuron had jumped 30- to 80-fold, and the synapse-to-neuron ratio was greatest at lower neuronal densities (<500 neurons/mm$^2$; mean approximately 400 synapses/neuron) compared to mid and higher neuronal densities (500–4500 neurons/mm$^2$; mean of approximately 150 synapses/neuron) ($p<0.05$). These results suggest a relationship between neuronal density and synapse number that may have implications in the neurobiology of developing neuronal networks as well as processes of cell death and regeneration.



## 1. Introduction

Synapses are the fundamental units of interneuronal communication, and the formation and maintenance of these relays are crucial elements of neuronal function. Synaptogenesis occurs throughout the entire life span of an organism, including during development, at maturity, and with age (Eastwood et al., 1994, 2006; Martin-Pena et al., 2006). Moreover, these stages contain vastly different and continuously evolving numbers of mature neurons (Paizanis et al., 2007; Pakkenberg et al., 2003; Seeger et al., 2005). For instance, development of the nervous system involves significant neuronal loss, and this developmental pruning is

* *Corresponding author*. Center for Brain Injury and Repair, Department of Neurosurgery, University of Pennsylvania, 105 Hayden Hall / 3320 Smith Walk, Philadelphia, PA 19104, USA.
E-mail address: dkacy@mail.med.upenn.edu (D.K. Cullen).
[1] The first two authors contributed equally to this work.

0006-8993/$ – see front matter © 2010 Elsevier B.V. All rights reserved.
doi:10.1016/j.brainres.2010.08.058

accompanied by an increase in synaptogenesis (Oppenheim, 1991; Waimey and Cheng, 2006). Human aging involves further neuronal loss, and although the overall loss in the human cerebral cortex may be as little at 10% (Pakkenberg et al., 2003), this phase is also characterized by synaptic plasticity (Waimey and Cheng, 2006). In addition, there are differences in neuronal and synaptic density across species that may provide insight into relationships between these parameters. For example, although the mature human cerebral cortex has one-fifth the neuronal density as found in the mouse, there is at least two times the number of synapses per neuron (DeFelipe et al., 2002). Thus, the observed decreases in neuronal density with aging and across species appear to correlate with increases in the number of synapses per neuron; however, it is not clear whether this increase in the synapse-to-neuron ratio is an adaptive response based on decreased neuronal density or a preprogrammed function occurring independent of changes in neuronal density.

In addition, neural cell culture models have become invaluable in characterizing neuron behavior in a simplified, highly controlled setting, and thus are in widespread use. In these settings, cell density is often established based on experimental objectives. For example, low-density cultures may be used to evaluate dendritic spines or to visualize neurite outgrowth over long distances, whereas high-density cultures are often used for electrical interface via multielectrode arrays. However, the importance of neuronal density on development and function *in vitro* has previously been noted. For instance, using multielectrode arrays, neuronal cultures were shown to exhibit varying levels of electrical bursting dependent on plating density; neurons plated at a higher density (2500 cells/mm$^2$) exhibited higher levels of electrical bursting than sparser cultures (600 cells/mm$^2$) (Wagenaar et al., 2006). In addition, plating density may influence the rate of neuronal maturation, as population-based bursting was initially recorded at an earlier day *in vitro* (DIV) in cultures plated at higher density versus lower density (Wagenaar et al., 2006). In another culture system, high-density rat hippocampal neuronal cultures exhibited greater neurite extension than lower-density cultures, suggesting that contact between cells influences neurite outgrowth (van den Pol et al., 1998). In addition, at very early culture time points (3–4 DIV), higher-density neuronal cultures exhibited a three-fold increase in synapse formation than low-density cultures, implicating the distance that axons/dendrites must traverse to reach a target in the rate of synaptogenesis *in vitro* (van den Pol et al., 1998). While these studies provide evidence that neuronal density influences network electrophysiological behavior and initial synaptogenesis, the influence of neuronal density on the number of synapses per neuron in immature versus mature cultures has not been studied.

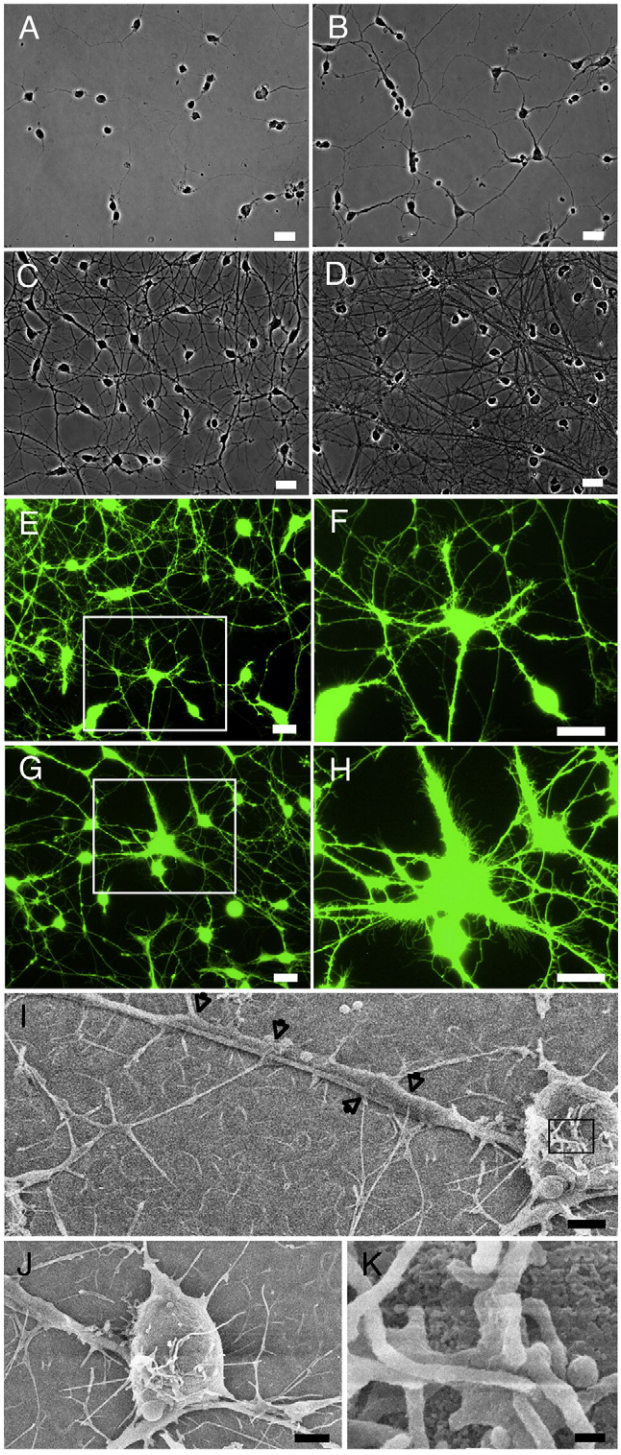


**Fig. 1 – Neuronal network development and putative synaptic junctures. Phase-contrast photomicrographs showing neurite extension and neuronal network formation from 2 DIV (A), 4 DIV (B), 8 DIV (C), and 14 DIV (D) at densities of 250–400 neurons/mm$^2$ (scale bars = 20 μm). Fluorescent micrographs of neuronal cultures at 8 DIV labeled with calcein AM to label live cells green (E–H) (scale bars = 20 μm). In these low-density cultures, evidence of robust neuritogenesis and active network development can be seen at this time point. Electron micrographs of low-density neuronal culture at 7 DIV (I–K). Perspective view of a large neuronal projection with neuritic contacts at regular intervals (arrows), representing points of potential synapses (I) (scale bar = 2 μm). Top view of neuron showing neuritic growth over the somatic surface (J) (scale bar = 2 μm). Expanded view of soma showing neurites growing over surface with intimate contact points representing potential synaptic junctures (K) (blown up view of boxed region in (I); scale bar = 200 nm).**

Accordingly, the goal of this study was to utilize an *in vitro* model to assess the influence of neuronal density and maturity on the number and distribution of synapses. Cerebral cortical neurons were plated in planar culture at densities ranging from 10 to 5000 neurons/mm$^2$ and neuronal and synaptic densities were evaluated over 21 DIV. The higher end of this density range approaches the neuron-to-neuron spacing found in specific layers in the cerebral cortex. In addition, higher neuronal densities correspond to decreased interneuronal distances and increased number of potential synaptic contacts in intimate proximity. Therefore, we hypothesized that in mature neuronal cultures, the number of synapses per neuron would increase with increasing neuronal density. Overall, we sought to determine whether inherent organizational principles dictated neuronal responses to various density environments that, in turn, directly influenced synapse formation and maintenance.

## 2. Results

### 2.1. *Neuronal culture development, survival, and functionality*

Cultures generated using cortical neurons extended multiple neurites per neuron with increasing neurite outgrowth over the first week in culture. Neurons formed an interconnected network by 8 DIV (Figs. 1A–C). At this time point, signs of neuritogenesis and neuritic spines were evident, indicating continued neurite outgrowth and further network development (Figs. 1E–H). Indeed, neuritic density increased substantially out to 14 DIV (Fig. 1D). In addition, neuronal morphology and the spatial distribution of cell–cell interactions were qualitatively assessed through low-voltage, high-resolution SEM. This analysis revealed neuritic–neuritic and neuritic–somatic junctures, representing sites of potential synapses (Figs. 1I–K). From 7 to 21 DIV, culture viability significantly decreased from 88.1±2.8% to 65.0±6.3% ($p<0.05$), indicating a degree of network pruning as the neuronal cultures matured. Moreover, dead cells typically presented as extremely condensed nuclei, permitting accurate morphological identification.

Fluorescent immunocytochemistry and confocal microscopy revealed tau$^+$ cells presenting synapsin staining distributed in discrete puncta along processes and somata (Figs. 2A–C). This distribution of presynaptic terminals colocalized with tau$^+$ neurites suggests the presence of active synapses (Fletcher et al., 1991; Hartley et al., 1999; O'Shaughnessy et al., 2003). In addition, whole-cell patch clamp recording demonstrated that neurons in culture exhibited excitable membrane properties including spontaneous and evoked action potentials (Fig. 2D). Neurons were observed to have typical resting membrane potentials. There was also evidence of probable inhibitory and excitatory postsynaptic potentials (Fig. 2D) as well as bursting (data not shown).

Thus, over 21 DIV, neurons in these cultures exhibited extensive process outgrowth, maintained viability, expressed mature isoforms of neuronal-specific cytoskeletal proteins, and demonstrated network connectivity. Electrophysiologically, neurons in culture had normal resting membrane potentials and exhibited spontaneous excitable properties, including the generation of action potentials and evidence of synaptic connections. Collectively, these observations provide significant evidence of network electrophysiological properties and that synapsin$^+$ puncta represent functional synapses.

### 2.2. *Neuronal percentage depends on DIV but not on plating density*

At 7 and 21 DIV, the vast majority of cells assumed neuronal, neurite-bearing morphologies across all culture densities. The neuronal presence (%) and density (#/mm$^2$) were assessing based on tau immunolabeling with nuclear counterstain. The percentage of tau$^+$ cells was calculated relative to the population of *live* cells to normalize for decreased survival at 21 DIV. At 7 DIV, the mean neuronal component across all plating densities was 91.5±14.2%. By 21 DIV, the overall neuronal presence had significantly decreased to 83.6±8.6% ($p<0.05$) (Fig. 3). Also, by 21 DIV, there was a substantial increase in neurite outgrowth, indicating that the surviving neurons were healthy. The neuronal presence did not statistically vary as a function of density at either 7 or 21 DIV; however, at 7 DIV, there was substantial variability in the percentage of tau$^+$ cells at extremely low plating densities (<100 neurons/mm$^2$). Longer-term neuronal survival was poor in these extremely low-density cultures, thus cultures at these densities were not evaluated out

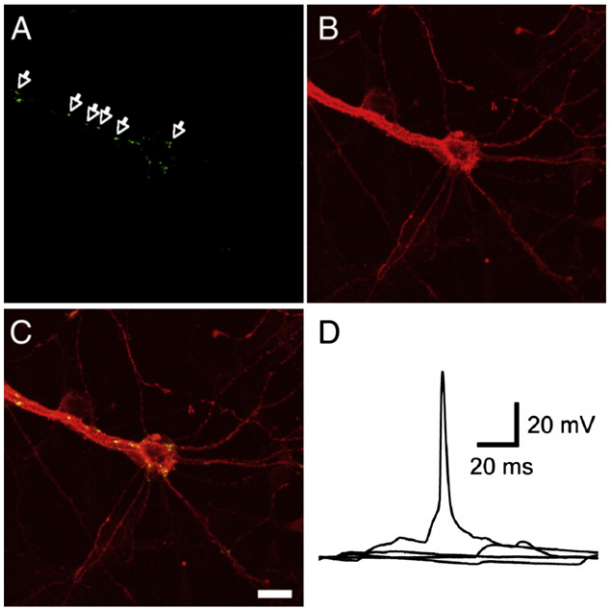


**Fig. 2 – Evidence of functional synapses and network activity. Confocal micrographs following immunocytochemistry for synapsin (green) (A) and tau (red) (B) with overlay (C), showing the distribution of synapsin$^+$ puncta along tau$^+$ neurites and soma at 14 DIV (scale bar=10 μm). Whole-cell patch clamp recordings were done on neurons in these planar cultures (D). Neurons exhibited synaptic potentials and spontaneous activity shown here as four successive traces in time in current clamp mode overlapped on the axis. Note the small excitatory synaptic potential steps with typical exponential shape leading to an action potential. Evidence of similar inhibitory potentials was observed but is not shown.**

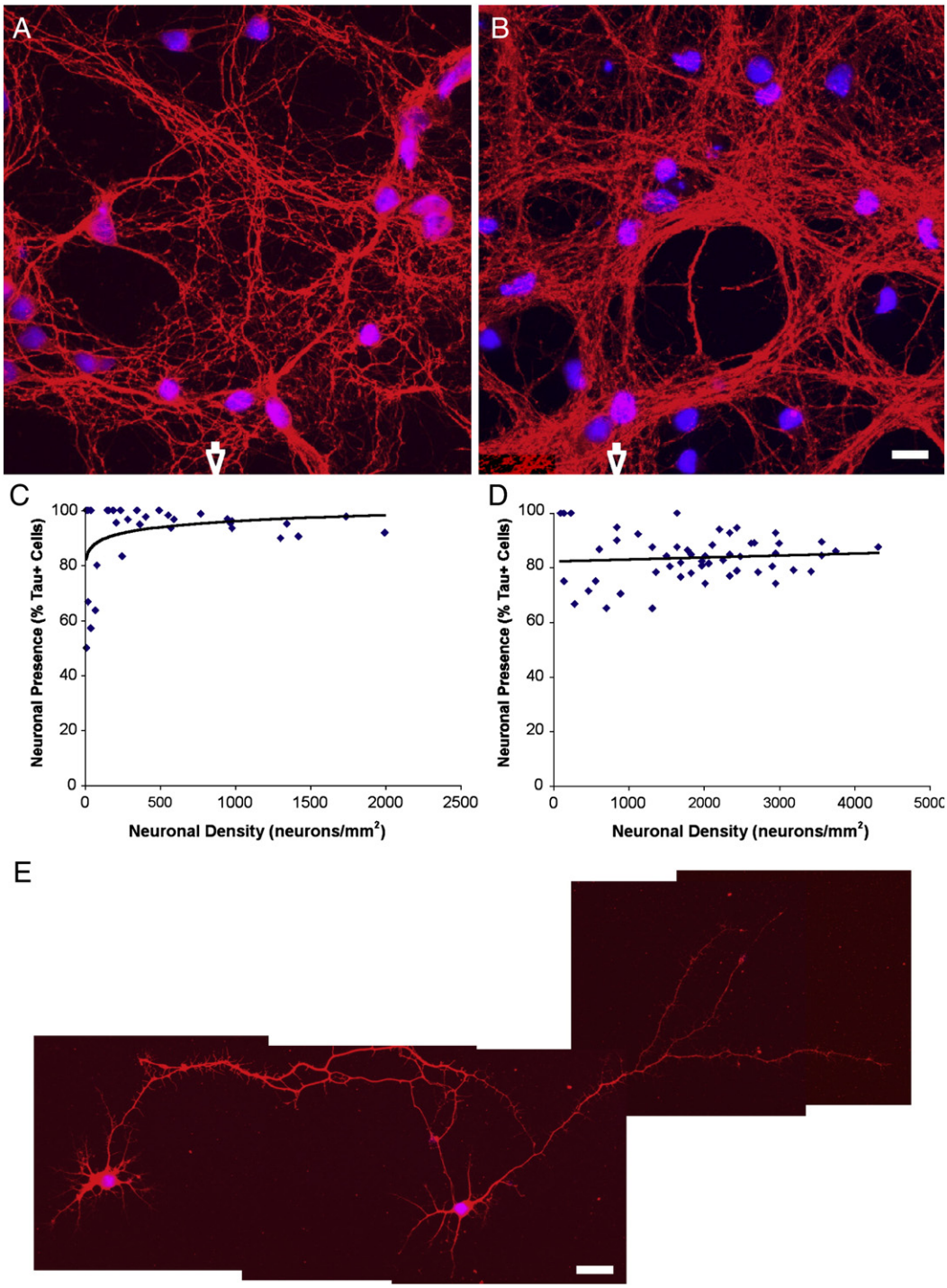


**Fig. 3 – The percentage of neurons as a function of the neuronal density (#/mm$^2$). The percentage of tau$^+$ cells was evaluated at 7 and 21 DIV in cultures across a range of neuronal densities. Representative confocal micrographs following immunocytochemistry for tau (red) with nuclear counterstain at 7 DIV (A) and 21 DIV (B) (scale bar = 10 μm). The neuronal presence did not vary significantly as a function of density at either 7 DIV (C) or 21 DIV (D); however, there was a significant decrease in the neuronal presence at 21 DIV compared to 7 DIV ($p < 0.05$). The neuronal density of each micrograph is denoted by the white arrows in (A) and (B) pointing to the *x* axes of (C) and (D), respectively. Example of an extremely low-density neuronal culture at 7 DIV (E) immunolabeled for tau (red) with nuclear counterstain (blue), demonstrating robust neurite outgrowth and typical morphology even under these culture conditions (scale bar = 20 μm). The growth of extremely low-density neuronal cultures is challenging, and data from such are often confounded by suboptimal health of the neurons.**

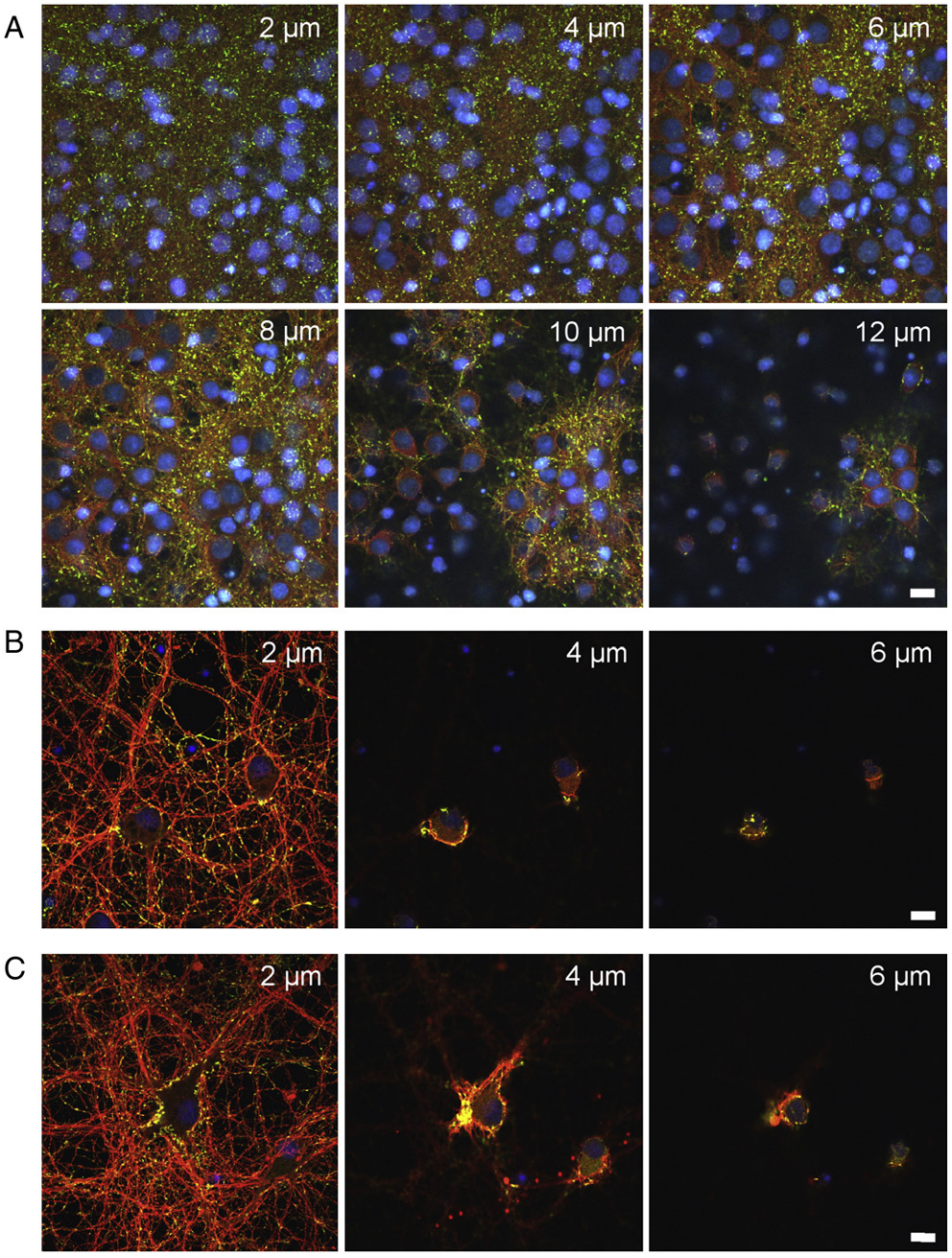


**Fig. 4 – Synaptic distribution at 21 DIV. Synapses were distributed across the height of the planar cultures at 21 DIV, as assessed by high-resolution confocal microscopy following immunocytochemistry for synapsin (green), tau (red), with nuclear counterstain (blue). Representative confocal micrographs with the height from the culture substrate denoted in the upper right-hand corner of each image (A–C). There were stark morphological and potentially voluminous differences between neurons in high-density (A) versus low-density (B–C) culture which corresponded to a >2-fold increase in culture thickness in high-density culture. This three-dimensional synaptic distribution, even in planar cultures, consisted of hundreds of synapses per neuron and demonstrated the complexity of the neuronal networks formed in culture. Scale bars = 10 μm.**

to 21 DIV. The decrease in neuronal presence from 7 to 21 DIV occurred with a concomitant increase in astroglial presence (data not shown). However, this astroglial presence was equivalent across plating densities, potentially making the influence of this factor consistent across different plating densities.

### 2.3. *Three-dimensional synaptic distribution in mature neuronal cultures*

High-resolution confocal microscopy revealed an elaborate three-dimensional distribution of neurites and synapses across the heights of high-density neuronal networks by 21 DIV.

Individual synapses were observed at discrete planes across the z-dimension of the cultures in both high- and low-density cultures at this time point (Fig. 4). The thickness of high-density cultures (3000–4500 neurons/mm$^2$) was 14.0±2.5 μm (range=11–18 μm). Interestingly, the overall culture thickness of low-density cultures (<500 neurons/mm$^2$) was 6.3±2.1 μm (range=4–10 μm), less than half of that in the high-density cultures ($p<0.001$). Moreover, neuronal somata in these low-density cultures had a much flatter morphology than neurons in high-density cultures. This analysis demonstrated the complex degree of spatial interactions present even in planar cultures that must be accounted for to accurately quantify synapses across the heights of these cultures.

### 2.4. *Synapse number depends on both DIV and plating density*

At 21 DIV, there was a considerable increase in the number of synapsin$^+$ puncta compared to 7 DIV (Fig. 5). At 7 DIV, the number of synapsin$^+$ puncta per area increased in a linear manner with increasing neuronal density ($R^2=0.92$), indicating that the number of synapses in culture increases with cell density (Fig. 6). However, the number of synapses per neuron did not vary based on neuronal density at this time point (Fig. 6). Specifically, at 7 DIV, there were no significant differences in the synapse-to-neuron ratio based on the various ranges of neuronal densities, with an overall mean of 4.6±1.2 synapses/neuron.

At 21 DIV, the number of synapsin$^+$ puncta per area increased approximately linearly with increasing neuronal density ($R^2=0.54$), although there was substantial variability (Fig. 7). However, the number of synapses per neuron decreased nonlinearly based on neuronal density at this time point (Fig. 7). At 21 DIV, the number of synapses per neuron was greatest at lower neuronal densities (<500 neurons/mm$^2$; 387.7±144.6 synapses/neuron) compared to mid and higher neuronal densities (500–4500 neurons/mm$^2$; 157.1±69.0 synapses/neuron) ($p<0.05$). There was considerable variability (63–569 synapses/neuron) over the different neuronal densities evaluated at 21 DIV. Overall, from 7 to 21 DIV, the number of synapses per neuron increased 80-fold in low-density cultures and 30-fold in mid- and high-density cultures ($p<0.001$).

## 3. Discussion

We evaluated the influence of neuronal density, and hence total neuronal number and interneuronal spacing, on synapse formation in developing and mature neuronal cultures. We utilized an *in vitro* model of cortical neurons in planar culture and analyzed the number of synapses based on immunolocalization of synapsin$^+$ puncta across varying neuronal densities. We made observations supporting that these synapsin$^+$ puncta represent functional synapses between neurons in these cultures. These observations include (1) network connectivity: extensive neurite outgrowth with identifiable neuritic–neuritic and neuritic–somatic junctures; (2) neuronal maturation: the expression of mature isoforms of neuron-specific cytoskeletal proteins; (3) synaptic distribution: synaptic marker distributed in discrete puncta along neurites/somata positive for a neuronal marker; and (4) electrophysiological parameters: excitable membrane properties including the generation of spontaneous and evoked action potentials and evidence of synaptic potentials.

A standard methodology to quantify synapses involves the utilization of transmission electron microscopy with the morphological identification of presynaptic terminals with appropriate vesicle levels/distributions and the presence of an opposing postsynaptic specialization. Although this methodology may be suitable to assess the efficacy of synapses, it may have inherent inaccuracies when quantifying the total number of synapses in our system due to variations in culture thickness based on neuronal density and the inhomogeneous synaptic distribution across the heights of these cultures. Therefore, we

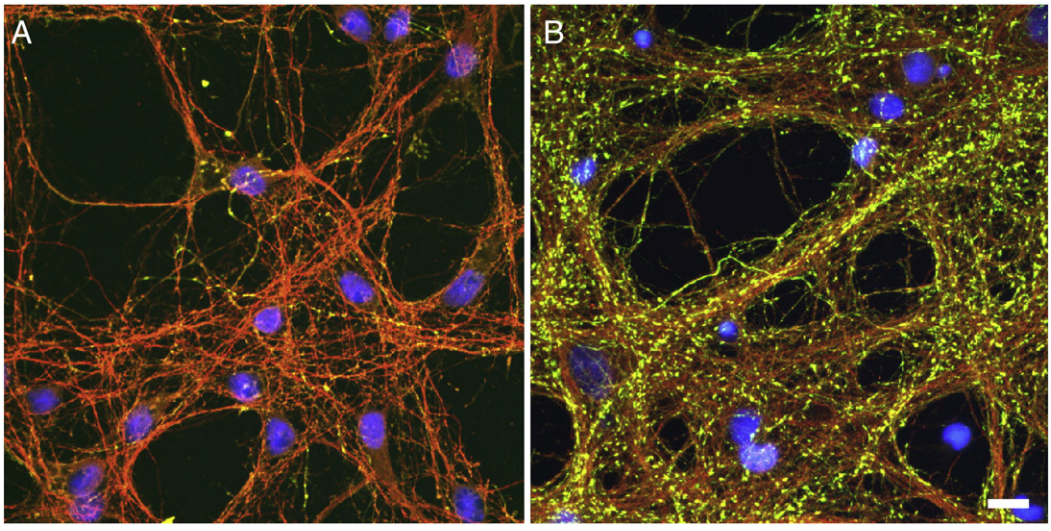


**Fig. 5 – Synapses per neuron based on neuronal density at 7 and 21 DIV. Representative confocal micrographs of neuronal cultures at 7 DIV (A) and 21 DIV (B) at approximately the same neuronal densities immunolabeled for synapsin (green), tau (red), with nuclear counterstain (blue). There were stark increases in the density of synapses at 21 DIV versus 7 DIV. Scale bar=10 μm.**

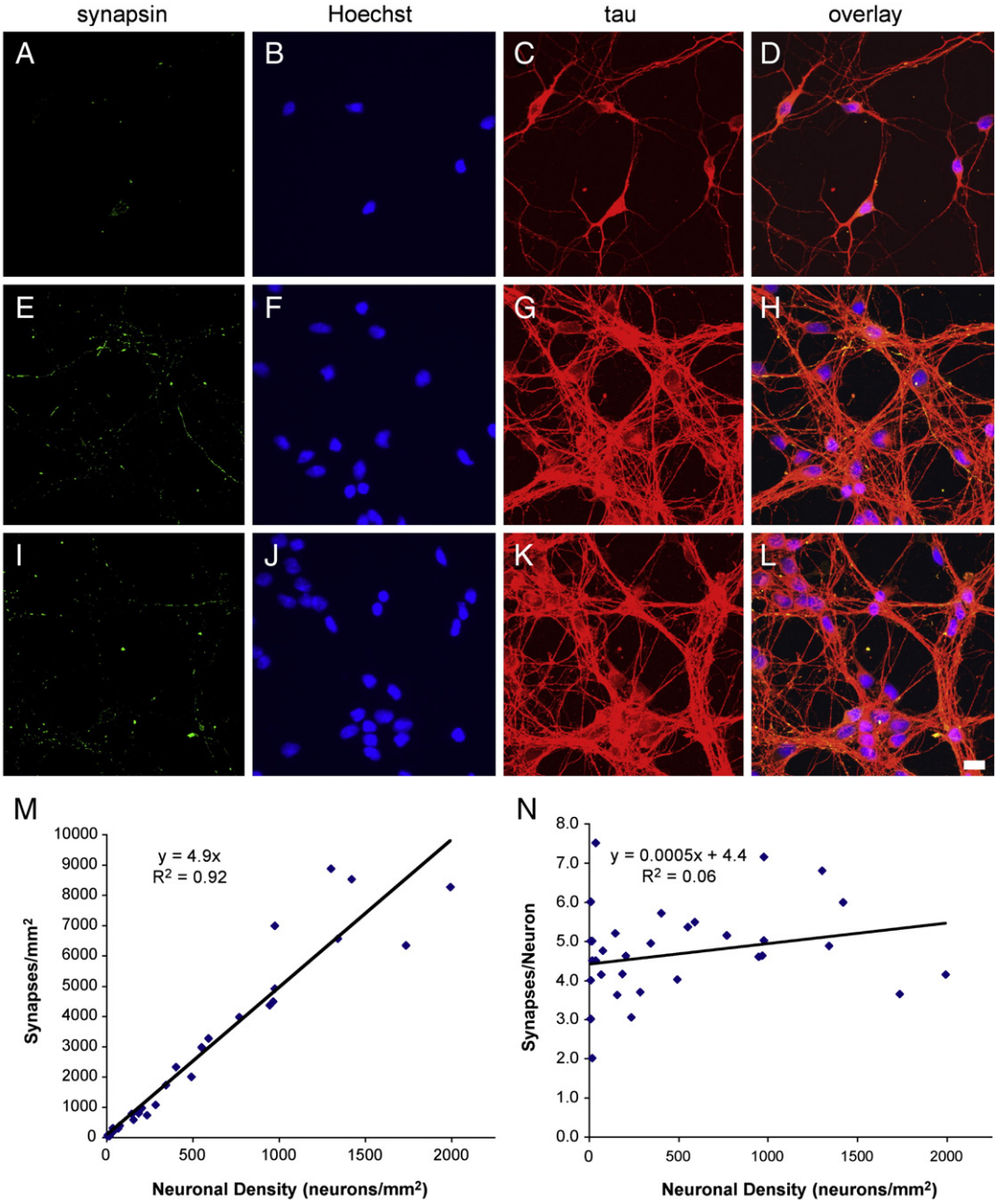


**Fig. 6 – Synapse-to-neuron ratio as function of neuronal density at 7 DIV. Representative confocal micrographs following immunocytochemistry for synapsin (green), tau (red) with nuclear counterstain (blue) for cultures at ~250 neurons/mm$^2$ (A–D), ~1000 neurons/mm$^2$ (E–H), and ~1500 neurons/mm$^2$ (I–L). At 7 DIV, the number of synapsin$^+$ puncta per area increased in a linear manner with increasing neuronal density ($R^2$=0.92) (M). However, the number of synapses per neuron did not vary based on neuronal density at this time point (N). Scale bar=10 μm.**

chose to quantify synapses based on the identification of synapsin$^+$ puncta using high-resolution full-thickness confocal microscopy scans (thus sampling across *x* and *y* with quantification across *z*). Using this methodology, we assessed the synapse-to-neuron ratio and distribution of synapses based on immunoreactivity for synapsin I. In the brain, it has been demonstrated that virtually all synapses contain synapsin I, with the only exceptions being neurons in highly specialized regions (De Camilli et al., 1983; Mandell et al., 1992; Moore and Bernstein, 1989; Stone et al., 1994). This finding was extended using hippocampal neurons *in vitro*, where it was demonstrated that in mature cultures, synapsin I distributed in discrete puncta was restricted to axonal varicosities containing large clusters of vesicles which were in intimate contact with opposing neuronal somata or dendrites, requisite properties of presynaptic specializations (Fletcher et al., 1991). Conversely, this same study demonstrated that synapsin I distribution was not a reliable indicator of synapses early in culture development, when

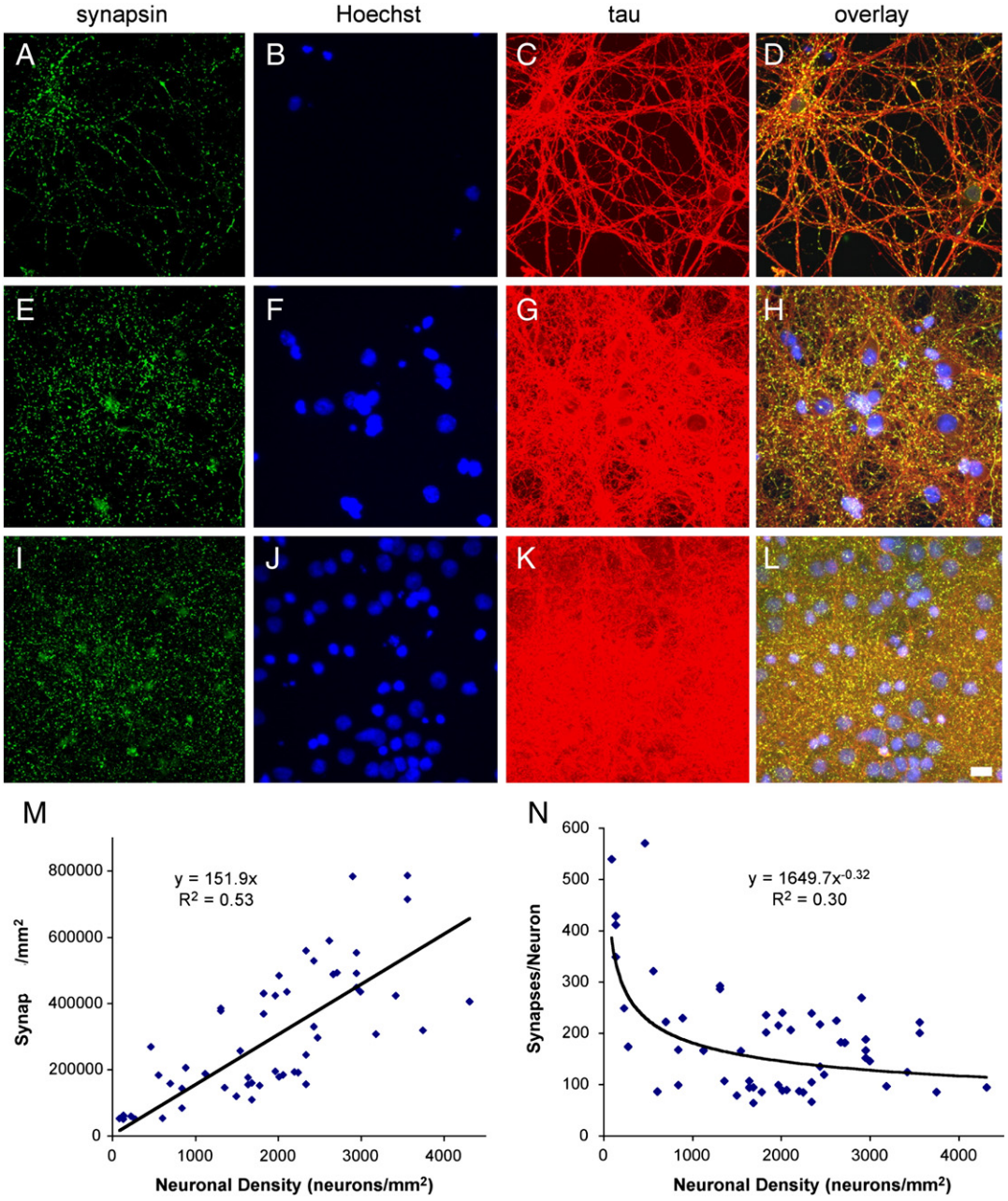


**Fig. 7 – Synapse-to-neuron ratio as function of neuronal density at 21 DIV. Representative confocal micrographs following immunocytochemistry for synapsin (green), tau (red) with nuclear counterstain (blue) for cultures at ~100 neurons/mm$^2$ (A–D), ~1000 neurons/mm$^2$ (E–H), and ~3000 neurons/mm$^2$ (I–L). Although there was substantial variability, the number of synapsin$^+$ puncta per area increased approximately linearly with increasing neuronal density ($R^2$=0.54) (M). However, the number of synapses per neuron decreased nonlinearly based on neuronal density at this time point (N). Scale bar=10 μm.**

neurites had yet to reach a target, as synapsin staining was distributed granularly and did not correlate with focal accumulation of vesicles. Thus, previous evidence supports that, in mature neuronal cultures, synapsin I distributed in discrete puncta in axons terminating at identifiable neuritic or somatic junctures is a reliable marker of pre-synaptic specializations in most cases.

In the current study, we observed presynaptic terminals aligned with tau$^+$ neurites/somata at both 7 and 21 DIV across all neuronal densities evaluated. At 7 DIV, the density of these synapsin$^+$ puncta was significantly greater in high-density cultures than low-density cultures; however, the number of synapsin$^+$ puncta per neuron did not vary with neuronal density. In mature cultures (21 DIV), the synapse-to-neuron ratio had increased 80-fold in low-density cultures and increased 30-fold in mid- and high-density cultures compared to immature cultures. At 21 DIV, the density of synapsin$^+$ puncta increased with neuronal density, but the number of synapses

per neuron decreased with increasing neuronal density before leveling off at higher neuronal densities. We originally hypothesized that in mature neuronal cultures, the synapses-to-neuron ratio would increase with increasing neuronal density. However, based on these results, we were compelled to reject this hypothesis. Our data demonstrate an inverse relationship between neuronal density and the ratio of synapses-to-neurons, although this trend levels off at the highest densities evaluated. Thus, developing neuronal populations in planar culture *in vitro* appear to recapitulate the inverse relationship between synapse-to-neuron ratio and neuronal density that has been reported in some cases *in vivo* (DeFelipe et al., 2002; Oppenheim, 1991; Waimey and Cheng, 2006). In addition, these general trends have been reported in mature and aged neuronal cultures, where neuronal density decreased over weeks in culture while synaptic density or synaptic marker levels remained constant (Ichikawa et al., 1993; Lesuisse and Martin, 2002). It should be noted that the higher cell densities evaluated in the current study represent the highest cell densities attainable in planar culture. In future work, these studies may be expanded to include three-dimensional (3-D) neuronal cultures capable of providing a neuronal density and distribution more similar to that found *in vivo* (Cullen et al., 2007c; Vukasinovic et al., 2009). Using these 3-D engineered systems, the effects of cellular constituents (Cullen et al., 2007b; Irons et al., 2008), extracellular matrix composition (Cullen et al., 2007a), or traumatic loading (Cullen and LaPlaca, 2006; LaPlaca et al., 2005) on synaptogenesis may systematically be evaluated.

In contrast to conventional wisdom that more neurons in culture will translate into more synaptic partners per neuron, we found that the synapse-to-neuron ratio progressed independently of neuronal density in immature cultures but was enhanced in low-density mature cultures. In a seminal study by Fletcher et al. (1994), the effects of neuronal plating density on synaptic density was directly investigated using hippocampal neurons, revealing more synapses per cell at higher cell densities. However, in addition to methodological differences related to neuronal culture conditions and initial plating densities, the analysis in this study was completed at 7 DIV. Hence, their longest time point was still based on neuronal cultures not considered fully mature. The idea that there will be more synapses per neuron at higher plating densities in mature cultures may be partly based on an extrapolation from the finding of Fletcher et al.; however, it is noteworthy that our finding challenges this extrapolation, not the validity of their original findings. This underscores the importance of DIV, and hence neuronal "maturation," in examining synapse formation, maintenance, and efficacy. The continuum transition from an immature to a mature neuronal phenotype is marked by established cellular polarity and electrochemical activity (i.e., synaptic communication). These events coincide with the widespread expression of mature isoforms of structural proteins as opposed developmental (immature) isoforms (Steinschneider et al., 1996). In addition, in immature neurons, GABA currents are excitatory, but later transition to become inhibitory (Ben-Ari et al., 1994; Cancedda et al., 2007; Chen et al., 1996; Deng et al., 2007; Ouardouz and Sastry, 2005). In particular, we choose 7 DIV as our early experimental time point as these neurons have a rich degree of axonal-dendritic and axonal–somatic connectivity, yet are still considered immature (e.g., GABA currents are not yet inhibitory, cytoskeletal proteins are lighter isoforms, etc.). However, by approximately 14 DIV, neurons are typically considered mature, thus our 21 DIV time point represented mature cultures. At these discrete time points, we quantified the number of neurons ($tau^+$ cells) and the number of synapses ($synapsin^+$ puncta) for a region-of-interest, thus the calculated synapse-to-neuron ratio was a composite representation for a particular observed region rather than the precise number of synapses made by a particular neuron. Other methodologies that only evaluate synaptic density based on the desired cell plating density may fail to account for local variation in neuronal density and changes in neuronal density due to network pruning. Thus, these approaches fail to normalize based on relevant culture alterations and may not accurately capture potential changes in neuronal response based on culture density and maturity.

Factors other than neuronal density and maturation may influence the interpretation of the current study, such as astroglial presence and neurotrophin concentrations. Neurons in culture form functional synapses when grown with or without astrocytic support, but changes in astroglial presence have been shown to affect synapse formation and density (Boehler et al., 2007; Hartley et al., 1999). In our current experiment, we had only a modest astrocytic presence; however, previous work in our lab has shown that cortical neurons in coculture with astrocytes (1:1 plating ratio) result in a >2-fold increase in the synapse-to-neuron ratio at matched neuronal densities and DIV as used in the current study (data not shown). Moreover, the effects of astrocytic presence on synaptogenesis may be evaluated within 3-D matrices (Irons et al., 2008). In addition to influencing interneuronal distances and the number of synaptic partners in close contact, neuronal density also influences trophic factor concentrations and availability (van den Pol et al., 1998). Neurotrophic factors are involved in regulation of survival, neurite outgrowth, and synapse formation/plasticity in developing as well as mature neuronal networks (Oppenheim, 1991; Sayer et al., 2002; Waimey and Cheng, 2006). Although we focused on the influence of neuronal density on synapse formation in predominantly neuronal populations, thus varying the degree of neuron-neuron contact and interneuronal spacing, the influences of astroglial support and neurotrophin concentrations should also be noted.

The results of this study may be applicable to models of development and aging since both the central and peripheral nervous systems exhibit changes in neuron number and maturity with increasing age (Oppenheim, 1991). Development of the nervous system involves significant neuronal and axonal loss, which occurs during and following phenotypic differentiation of defined neuronal populations, and this developmental pruning is accompanied by an increase in synaptogenesis (Oppenheim, 1991; Waimey and Cheng, 2006). Also, there is a link between synaptic activity and neuronal death, as the suppression of synaptic transmission during neural development was found to reduce neuron death, and conversely, increased synaptic activity increased the rate of neuronal death (Oppenheim, 1991). Organisms must utilize different strategies to cope with neuronal loss throughout the life span. For instance, human aging involves neuronal death; there are reports of up to nearly 50% loss of neurons in various regions of the brain by age 60 (Cabello et al., 2002); however, overall neuronal loss in the human cerebral

cortex may be as little at 10% (Pakkenberg et al., 2003). This type of neuronal loss is also characterized by synaptic plasticity, which may serve to maintain functionality by increasing the number of synapses per neuron (Waimey and Cheng, 2006). In addition, in the mouse somatosensory cortex (layers II/III) of neonates compared to adults, there was a 35% reduction in neuronal density concomitant with a five-fold increase in the synaptic density. This resulted in less than 250 synapses per neuron in high-density immature brains but close to 5000 synapses per neuron in low-density mature brains, approximately a 20-fold increase (Seeger et al., 2005). Long-term neuronal culture may provide a platform to analyze changes in the synapse-to-neuron as a function of neuronal aging (Lesuisse and Martin, 2002).

Interestingly, species-specific differences in synapse-to-neuron ratio correlate with changes in neuronal density. For instance, the neuronal densities in mature human versus mouse cerebral cortices were reported to be approximately 25,000 neurons/mm$^3$ and 120,000 neurons/mm$^3$, respectively; however, this nearly five-fold increase in neuronal density between humans and mice was accompanied by over a 50% reduction in the number of synapses/neuron (DeFelipe et al., 2002). Thus, although humans have decreased neuronal densities, there are increased numbers of synapses per neuron compared to mice. Reduced *in vitro* models may lend insight into environmental parameters that result in changes in the number of synapses per neuron, a potential compensatory mechanism employed by neuronal networks to deal with low neuronal densities.

Previous reports have noted the influence of neuronal density on ensemble electrophysiological behavior and early synaptogenesis and neurite outgrowth. In immature developing neuronal cultures (3–4 DIV), neurite outgrowth was enhanced (based on neurite length and growth rate) in higher density compared to low-density cultures, specifically implicating neuron–neuron contact (i.e., increased availability of membrane surface area for axonal guidance) in this enhanced neurite outgrowth (van den Pol et al., 1998). These neuronal cultures exhibited GABA and glutamate release, indicative of synaptogenesis, after 3–4 DIV in high-density cultures but not in low-density cultures at this time point (van den Pol et al., 1998). Enhanced neurite outgrowth in higher density cultures was thought to increase the probability of synapse formation and thus explained the finding that the total synapses in these cultures increased with neuronal density at this early time point. Thus, the distance an axon must grow to find a postsynaptic partner plays a substantial role in the timing of synapse formation, although based on the results of the current study, these differences appear to be overcome on a per-neuron basis by 7 DIV and indeed are maintained out to 21 DIV. In addition, neuronal cultures were shown to exhibit varying levels of population-based electrical bursting depending on plating density, with more bursting found in higher-density cultures and at an earlier time point (Wagenaar et al., 2006). Taken together, these results suggest that high-density neuronal cultures may mature faster, which may influence the rate of synaptogenesis and synaptic maintenance/plasticity.

Future extensions of this work may determine whether increased synaptic input (via multielectrode arrays or exogenous neurotransmitter stimulation) influences neuronal pruning and/or the changes in the synapse-to-neuron ratio observed to develop over 7 to 21 DIV. Moreover, previous reports from the *in vivo* cerebral cortex have noted that (1) increased soma size/volume correlates with increased dendritic complexity and axonal enlargement and (2) that the number of synaptic sites remains fairly constant along dendrites and axons (Gutierrez-Ospina et al., 2004; Seeger et al., 2005). Thus, an interesting future extension of this work would be to evaluate whether *in vitro* neuronal networks recapitulate these relationships by quantifying whether larger neuronal somata with increased arborization are found in lower-density versus higher-density cultures. In addition, the effects of neuronal density on the synapse-to-neuron ratio for particular broad neuronal subtypes (e.g., pyramidal vs. nonpyramidal, inhibitory vs. excitatory) would be interesting, as differential responses may be observed across subtypes.

In summary, this work evaluated mechanisms employed by developing neuronal networks to respond to varying neuronal densities by modulating the number of synapses per neuron. Our findings suggest that neuronal populations inherently respond to low neuronal density environments by increasing the number of synapses per neuron. The influence of neuronal density on inherent self-organizational properties such as synapse formation and network development has implications for the *in vitro* study of neurobiological phenomena and is critical to the accurate application and interpretation of such reduced models. Moreover, these inherent neuronal properties may have implications in the neurobiology of development and aging as well as responses to neurotrauma or neurodegenerative disorders.

## 4. Experimental procedures

### 4.1. *Cell culture*

All procedures involving animals were approved by the Institutional Animal Care and Use Committee of the Georgia Institute of Technology and followed the National Institutes of Health Guide for the Care and Use of Laboratory Animals (NIH Publication No. 86-23; revised 1985). Cerebral cortices were isolated from embryonic day 18 rat fetuses (Sprague-Dawley; Charles River, Wilmington, MA), digested in trypsin (0.25%)+1 mM EDTA (Invitrogen, Carlsbad, CA), and separated using a flame-narrowed Pasteur pipette as described previously (Cullen and LaPlaca, 2006). Following centrifugation (100 ×*g*), the cells were suspended in a defined medium (Neurobasal+2% B-27+500 μM L-glutamine (Invitrogen)). The resulting single-cell neuronal suspensions were plated at densities ranging from 10 to 5000 cells/mm$^2$ on glass slides pretreated with poly-L-lysine (0.05 mg/mL; Sigma-Aldrich, St. Louis, MO). This procedure yields a nearly pure neuronal population with <1% astroglial presence (Brewer et al., 1993; Brewer, 1995). Cultures were maintained at 37 °C and 5% $CO_2$–95% humidified air, and the medium was replaced at 24 hours and every 2 days thereafter.

### 4.2. *Cell staining*

Culture viability was assessed by incubation with markers of live (calcein AM; 2 μM) and dead/dying cells (ethidium homodimer-1 (EthD-1); 4 μM) (Molecular Probes, Eugene, OR) at 37 °C for 30 min and then rinsed with 0.1 M Dulbecco's phosphate-buffered saline

(DPBS; Invitrogen). For immunocytochemistry, cultures were fixed in 3.7% formaldehyde (Fisher, Fairlawn, NJ) for 30 min, rinsed in PBS and permeabilized using 0.3% Triton X-100 plus 4% goat serum (Invitrogen) for 20 min. Primary antibodies were added (in PBS+4% serum) at 37 °C for 4 hours. After rinsing, secondary fluorophore-conjugated antibodies (Alexa 488- or 546-conjugated IgG; Molecular Probes) in PBS plus 4% serum were added at 18–24 °C for 2 hours. Cultures were immunolabeled with primary antibodies recognizing tau-5, a microtubule-associated protein expressed primarily in neurons (Binder et al., 1985; Goedert et al., 1991) (MS247P, 1:200; NeoMarkers, Fremont, CA) and synapsin I, a synaptic vesicle protein localized in presynaptic specializations (Fletcher et al., 1991) (A6442, 1:200; Molecular Probes). Nuclear counterstaining was performed using Hoechst 33258 (1:1000; Molecular Probes). For scanning electron microscopy (SEM), cultures were fixed using 2.5% EM-grade glutaraldehyde in 0.1 M cacodylate buffer (pH 7.4) at 4 °C for 24 hours, washed in di-$H_2O$, and then postfixed with 1% $OsO_4$ in 0.1 M cacodylate buffer (pH 7.4) for 1 hour followed by several rinses. Cultures were dehydrated using ethanol (30, 50, 70, 3×100%, 15 min each) and wrapped in parafilm, and a critical point dryer (Polaron E-3000) was used for $CO_2$ exchange, phase transition, and subsequent release. Specimens were sputter coated with 3 nm of chromium before SEM.

### 4.3. *Whole-cell patch clamp*

For patch clamp recordings, borosilicate glass electrodes with filaments (external diameter 1.5 mm; inner diameter 0.75 mm; Sutter Instruments, Novato, CA) were pulled on a laser puller (P-2000; Sutter Instruments) with a 7–10 MΩ resistance. Electrodes were back-filled with internal solution (140 mM K-gluconate, 10 mM HEPES, 5 mM KCl, 0.1 mM K-EGTA, pH 7.3; 315–325 mOsm). The external solution was artificial cerebral spinal fluid (aCSF) containing 119 mM NaCl, 2.5 mM KCl, 1.3 mM $MgCl_2$, 2.5 mM $CaCl_2$, 1 mM $NaH_2PO_4$, 26.2 mM $NaHCO_3$, and 11 mM glucose (pH 7.4 by continuously bubbling with $CO_2/O_2$ (95:5) mixture; 320 mOsm) made daily and gravity perfused at 1–2 mL/min. An AxoPatch 1D (Axon Instruments) amplifier, a Digidata acquisition card, and a WinWCP software were used for data acquisition, recording, and stimulating. Recordings were displayed on Tektronix Oscilloscopes (TDS 3014B and 7603) and analyzed offline in WinWCP and Igor Pro (WaveMetrics).

### 4.4. *Microscopy and data collection*

Cells were imaged using phase-contrast or fluorescent microscopy techniques on an epifluorescent microscope (Eclipse TE300; Nikon, Melville, NY) with images digitally captured (DKC5T5/DMC; Sony, Tokyo, Japan) and analyzed with Image-Pro Plus (Media Cybernetics, Silver Spring, MD). Alternatively, cells were fluorescently imaged using a confocal laser scanning microscope (LSM 510; Zeiss, Oberkochen, Germany), with scans acquired across the full thickness of cultures and analyzed using LSM Image Browser (Zeiss).

High-resolution confocal microscopy was utilized to quantify the neuronal presence and the number of synapsin$^+$ puncta. The neuronal presence (%) and neuronal density (#/mm$^2$) were assessed by determining the number of tau$^+$ cells with Hoechst counterstaining. The number of synapses (#/mm$^2$) was determined by quantifying synapsin$^+$ puncta across the thickness of the cultures. Specifically, in mid- and high-density cultures with synapsin$^+$ puncta at overlapping $x$–$y$ coordinates, multiple regions were subsampled across the z space. This was performed across the entire thickness of the region, with 2–3 μm plane-to-plane separation to ensure quantification of unique synapses. The number of synapses per neuron was calculated by dividing the density of synapsin$^+$ puncta with the density of tau$^+$ cells.

### 4.5. *Experimental design and statistical analyses*

Culture viability (%) was assessed in cultures plated at 1250–2500 cells/mm$^2$ at 7–8 DIV and 21 DIV by quantifying live cells (fluorescing green via AM cleavage) and dead cells (nuclei fluorescing red via EthD-1 binding) ($n$=5 cultures per time point; 3–5 observations per culture). Whole-cell patch clamp recording was performed at 1250–2500 cells/mm$^2$ at 21–35 DIV ($n$=27 cells from 15 cultures). At 7 and 21 DIV, the neuronal presence (%) and neuronal density (#/mm$^2$) were assessed, and the number of synapses (#/mm$^2$) was determined by quantifying synapsin$^+$ puncta ($n$=11 and $n$=19 cultures, respectively; 2–4 observations per culture). Regression analyses were used for best-fit to data at 7 and 21 DIV. To evaluate the influence of within-culture variations (based on neuronal density) on local synapse formation, neuronal density was isolated as the independent variable, and data were evaluated across within-culture observations (thus absorbing culture-to-culture variability). In addition, Student's $t$-tests were used for data groups combined based on density or DIV ($p<0.05$ required for significance). Data are presented as mean±standard deviation.

## Acknowledgments

This work was partially supported by NSF (CAREER Award BES-0093830), NIH/NIBIB (EB001014), and NSF (EEC-9731643). This work made use of shared facilities from the Georgia Tech/Emory Center (GTEC) for the Engineering of Living Tissues, an ERC supported under Award Number EEC-9731643. For assistance in electrophysiology studies, the authors thank Dr. Nevin A. Lambert (Department of Pharmacology and Toxicology, Medical College of Georgia, Augusta, GA). The authors also thank Victoria Tsai for technical assistance.

## REFERENCES

Ben-Ari, Y., Tseeb, V., Raggozzino, D., Khazipov, R., Gaiarsa, J.L., 1994. gamma-Aminobutyric acid (GABA): a fast excitatory transmitter which may regulate the development of hippocampal neurones in early postnatal life. Prog. Brain Res. 102, 261–273.

Binder, L.I., Frankfurter, A., Rebhun, L.I., 1985. The distribution of tau in the mammalian central nervous system. J. Cell Biol. 101, 1371–1378.

Boehler, M.D., Wheeler, B.C., Brewer, G.J., 2007. Added astroglia promote greater synapse density and higher activity in neuronal networks. Neuron Glia Biol. 3, 127–140.

Brewer, G.J., 1995. Serum-free B27/neurobasal medium supports differentiated growth of neurons from the striatum, substantia nigra, septum, cerebral cortex, cerebellum, and dentate gyrus. J. Neurosci. Res. 42, 674–683.

Brewer, G.J., Torricelli, J.R., Evege, E.K., Price, P.J., 1993. Optimized survival of hippocampal neurons in B27-supplemented neurobasal, a new serum-free medium combination. J. Neurosci. Res. 35, 567–576.

Cabello, C.R., Thune, J.J., Pakkenberg, H., Pakkenberg, B., 2002. Ageing of substantia nigra in humans: cell loss may be compensated by hypertrophy. Neuropathol. Appl. Neurobiol. 28, 283–291.

Cancedda, L., Fiumelli, H., Chen, K., Poo, M.M., 2007. Excitatory GABA action is essential for morphological maturation of cortical neurons in vivo. J. Neurosci. 27, 5224–5235.

Chen, G., Trombley, P.Q., van den Pol, A.N., 1996. Excitatory actions of GABA in developing rat hypothalamic neurones. J. Physiol. 494 (Pt 2), 451–464.

Cullen, D.K., LaPlaca, M.C., 2006. Neuronal response to high rate shear deformation depends on heterogeneity of the local strain field. J. Neurotrauma 23, 1304–1319.

Cullen, D.K., Lessing, M.C., Laplaca, M.C., 2007a. Collagen-dependent neurite outgrowth and response to dynamic deformation in three-dimensional neuronal cultures. Ann. Biomed. Eng. 35, 835–846.

Cullen, D.K., Simon, C.M., LaPlaca, M.C., 2007b. Strain rate-dependent induction of reactive astrogliosis and cell death in three-dimensional neuronal–astrocytic co-cultures. Brain Res. 1158, 103–115.

Cullen, D.K., Vukasinovic, J., Glezer, A., Laplaca, M.C., 2007c. Microfluidic engineered high cell density three-dimensional neural cultures. J. Neural Eng. 4, 159–172.

De Camilli, P., Cameron, R., Greengard, P., 1983. Synapsin I (protein I), a nerve terminal-specific phosphoprotein: I. Its general distribution in synapses of the central and peripheral nervous system demonstrated by immunofluorescence in frozen and plastic sections. J. Cell Biol. 96, 1337–1354.

DeFelipe, J., Alonso-Nanclares, L., Arellano, J.I., 2002. Microstructure of the neocortex: comparative aspects. J. Neurocytol. 31, 299–316.

Deng, L., Yao, J., Fang, C., Dong, N., Luscher, B., Chen, G., 2007. Sequential postsynaptic maturation governs the temporal order of GABAergic and glutamatergic synaptogenesis in rat embryonic cultures. J. Neurosci. 27, 10860–10869.

Eastwood, S.L., Burnet, P.W., McDonald, B., Clinton, J., Harrison, P.J., 1994. Synaptophysin gene expression in human brain: a quantitative in situ hybridization and immunocytochemical study. Neuroscience 59, 881–892.

Eastwood, S.L., Weickert, C.S., Webster, M.J., Herman, M.M., Kleinman, J.E., Harrison, P.J., 2006. Synaptophysin protein and mRNA expression in the human hippocampal formation from birth to old age. Hippocampus 16, 645–654.

Fletcher, T.L., Cameron, P., De Camilli, P., Banker, G., 1991. The distribution of synapsin I and synaptophysin in hippocampal neurons developing in culture. J. Neurosci. 11, 1617–1626.

Fletcher, T.L., De Camilli, P., Banker, G., 1994. Synaptogenesis in hippocampal cultures: evidence indicating that axons and dendrites become competent to form synapses at different stages of neuronal development. J. Neurosci. 14, 6695–6706.

Goedert, M., Crowther, R.A., Garner, C.C., 1991. Molecular characterization of microtubule-associated proteins tau and MAP2. Trends Neurosci. 14, 193–199.

Gutierrez-Ospina, G., Uribe-Querol, E., Sanchez, N., Geovannini, H., Padilla, P., Hernandez-Echeagaray, E., 2004. Similar synapse density in layer IV columns of the primary somatosensory cortex of transgenic mice with different brain size: implications for mechanisms underlying the differential allocation of cortical space. Brain Behav. Evol. 64, 61–69.

Hartley, R.S., Margulis, M., Fishman, P.S., Lee, V.M., Tang, C.M., 1999. Functional synapses are formed between human NTera2 (NT2N, hNT) neurons grown on astrocytes. J. Comp. Neurol. 407, 1–10.

Ichikawa, M., Muramoto, K., Kobayashi, K., Kawahara, M., Kuroda, Y., 1993. Formation and maturation of synapses in primary cultures of rat cerebral cortical cells: an electron microscopic study. Neurosci. Res. 16, 95–103.

Irons, H.R., Cullen, D.K., Shapiro, N.P., Lambert, N.A., Lee, R.H., LaPlaca, M.C., 2008. Three-dimensional neural constructs: a novel platform for neurophysiological investigation. J. Neural Eng. 5, 333–341.

LaPlaca, M.C., Cullen, D.K., McLoughlin, J.J., Cargill II, R.S., 2005. High rate shear strain of three-dimensional neural cell cultures: a new *in vitro* traumatic brain injury model. J. Biomech. 38, 1093–1105.

Lesuisse, C., Martin, L.J., 2002. Long-term culture of mouse cortical neurons as a model for neuronal development, aging, and death. J. Neurobiol. 51, 9–23.

Mandell, J.W., Czernik, A.J., De Camilli, P., Greengard, P., Townes-Anderson, E., 1992. Differential expression of synapsins I and II among rat retinal synapses. J. Neurosci. 12, 1736–1749.

Martin-Pena, A., Acebes, A., Rodriguez, J.R., Sorribes, A., de Polavieja, G.G., Fernandez-Funez, P., Ferrus, A., 2006. Age-independent synaptogenesis by phosphoinositide 3 kinase. J. Neurosci. 26, 10199–10208.

Moore, R.Y., Bernstein, M.E., 1989. Synaptogenesis in the rat suprachiasmatic nucleus demonstrated by electron microscopy and synapsin I immunoreactivity. J. Neurosci. 9, 2151–2162.

Oppenheim, R.W., 1991. Cell death during development of the nervous system. Annu. Rev. Neurosci. 14, 453–501.

O'Shaughnessy, T.J., Lin, H.J., Ma, W., 2003. Functional synapse formation among rat cortical neurons grown on three-dimensional collagen gels. Neurosci. Lett. 340, 169–172.

Ouardouz, M., Sastry, B.R., 2005. Activity-mediated shift in reversal potential of GABA-ergic synaptic currents in immature neurons. Brain Res. Dev. Brain Res. 160, 78–84.

Paizanis, E., Kelai, S., Renoir, T., Hamon, M., Lanfumey, L., 2007. Life-long hippocampal neurogenesis: environmental, pharmacological and neurochemical modulations. Neurochem. Res. 32, 1762–1771.

Pakkenberg, B., Pelvig, D., Marner, L., Bundgaard, M.J., Gundersen, H.J., Nyengaard, J.R., Regeur, L., 2003. Aging and the human neocortex. Exp. Gerontol. 38, 95–99.

Sayer, F.T., Oudega, M., Hagg, T., 2002. Neurotrophins reduce degeneration of injured ascending sensory and corticospinal motor axons in adult rat spinal cord. Exp. Neurol. 175, 282–296.

Seeger, G., Gartner, U., Arendt, T., 2005. Transgenic activation of Ras in neurons increases synapse formation in mouse neocortex. J. Neural Transm. 112, 751–761.

Steinschneider, R., Delmas, P., Nedelec, J., Gola, M., Bernard, D., Boucraut, J., 1996. Appearance of neurofilament subunit epitopes correlates with electrophysiological maturation in cortical embryonic neurons cocultured with mature astrocytes. Brain Res. Dev. Brain Res. 95, 15–27.

Stone, L.M., Browning, M.D., Finger, T.E., 1994. Differential distribution of the synapsins in the rat olfactory bulb. J. Neurosci. 14, 301–309.

van den Pol, A.N., Obrietan, K., Belousov, A.B., Yang, Y., Heller, H.C., 1998. Early synaptogenesis *in vitro*: role of axon target distance. J. Comp. Neurol. 399, 541–560.

Vukasinovic, J., Cullen, D.K., LaPlaca, M.C., Glezer, A., 2009. A microperfused incubator for tissue mimetic 3D cultures. Biomed. Microdevices 11, 1155–1165.

Wagenaar, D.A., Pine, J., Potter, S.M., 2006. An extremely rich repertoire of bursting patterns during the development of cortical cultures. BMC Neurosci. 7, 11.

Waimey, K.E., Cheng, H.J., 2006. Axon pruning and synaptic development: how are they per-plexin? Neuroscientist 12, 398–409.